Electrical and Photovoltaic Properties of Pb/*trans*-$(CH)_x$ and Pb/$[CH(AsF_5)_y]_x$ Schottky Barriers

E. VANDER DONCKT and J. KANICKI, *Chimie Organique Physique, Université Libre de Bruxelles, 50 Av. F. D. Roosevelt, 1050 Bruxelles, Belgium*, and P. FEDORKO, *Department of Physics, Electrotechnical Faculty, Slovak Technical University, Gottwaldovo nam.19, 81219 Bratislava, Czechoslovakia*

Synopsis

The rectifying and photovoltaic properties of Pb/*trans*-polyacetylene/graphite sandwich cells have been examined. The dependence of the short-circuit current density (J_{sc}) and open-circuit voltage (V_{oc}) on light intensity have been determined. Some data on a Pb/AsF_5 lightly doped polyacetylene graphite cell are also reported.

INTRODUCTION

Many organic materials such as polyvinylpyridines,[1] polypyrroles,[2] phthalocyanines,[3] and polyphenylacetylenes[4] are the subject of research aiming at the determination of their electrical properties and usefulness as materials for Schottky barriers and photovoltaic cells. Among the polymers, polyacetylene is actively investigated.[5–7]

In this paper, we report the first data on the rectifying and photovoltaic characteristics of Pb/*trans*-$(CH)_x$/graphite and Pb/*trans*-$[CH(AsF_5)_y]_x$/graphite devices. *Trans*-$(CH)_x$ and *trans*-$[CH(AsF_5)_y]_x$, respectively, stand for *trans*-polyacetylene and the lightly doped polymer. Electrical characteristics of the junctions with the doped polymer were unstable and displayed ageing effects within a few hours for y values >0.01. Therefore, the AsF_5 doping level had to be maintained at 0.005.

EXPERIMENTAL

The *trans*-polyacetylene films were synthesized following Shirakawa's technique.[8] The samples prepared during this work have similar properties (UV-visible–IR absorption spectra, C:H analysis, shiny aspect) to those described elsewhere.[9,10] Doped samples were made by leaving the films in contact with AsF_5 vapor until the desired doping level was obtained. The dopant concentration was determined by weight uptake. The films had a typical thickness of 50 μm.

The backside of the films was painted with Acheson Electrodag +502 (suspension of colloidal graphite) and the front side was covered with a semitransparent lead layer. The metal was deposited by evaporation under reduced pressure ($\sim 10^{-4}P$) with the help of a Leybold-Heraeus Univex 300 (Vacuum Coater).

Journal of Applied Polymer Science, Vol. 29, 619–627 (1984)
 CCC 0021-8995/84/020619-09$04.00

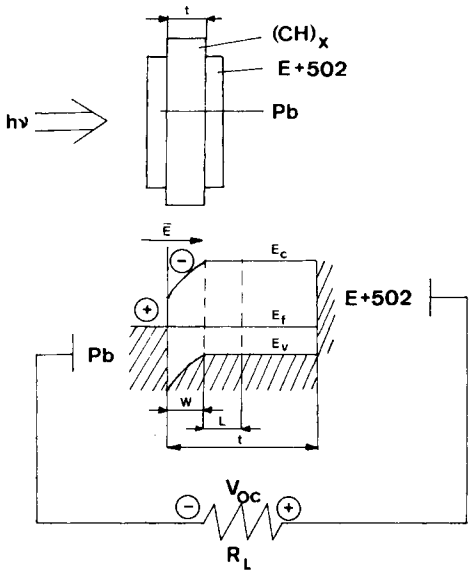

Fig. 1. Configuration of the sandwich cell and qualitative variation of the electrical potential along the cell: E_c = lower limit of the conduction band; E_f = Fermi energy level; E_v = upper limit of the valence band[14]; W = depletion layer; L = diffusion length of the carriers; $\bar{E}$ = electrical field; t = thickness of the polymer film.

The J–V characteristics were obtained with a Heathkit IP-2071 Power Supply; the voltages were measured with a Keithley 616 Digital Electrometer and the currents with a Solartron 7051 DVM.

The white light source was a Xenon 150W Illuminator powered by a Varian PS 150-8 Supply. A Unicam SP500 Monochromator was used for the experiments with monochromatic light. Irradiations were performed through the lead contact (Fig. 1).

RESULTS

As shown in Figure 2, doped and undoped polymers form rectifying contacts with lead. It was checked that for the current densities encountered during this work, the contact with Electrodag +502 is ohmic. The specific contact resistance was ~300 Ω·cm. Forward bias corresponds to a negative voltage at the Pb electrode; under illumination, the metal electrode becomes negative with respect to the back contact.

Current Density–Voltage (J–V) Data. The rectification ratio at 1 V is 250 for undoped polyacetylene; this ratio decreases upon doping with AsF_5. Extrapolation to $J = 0$ of the linear part of the forward characteristic yields a value for the contact potential:

$$V_c = 0.7V$$

A similar value is found for the Pb/$(CH)_x$ and the Pb/$[CH(AsF_5)_y]_x$ contacts. At forward bias (V_F) greater than V_c, the J_F–V_F characteristic becomes linear. From the slope, a series resistance R_s of 10^3 Ω is estimated for the junction with

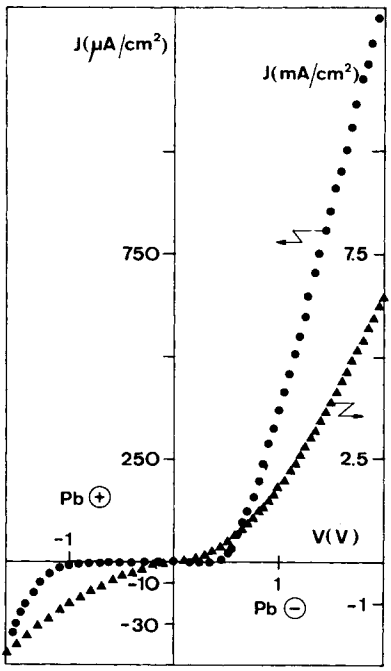

Fig. 2. Electrical characteristics of Pb/$(CH)_x$ (●) and Pb/$[CH(AsF_5)_y]_x$ cells (▲).

the undoped polymer. This corresponds to the bulk resistance of the polymer. The resistivity (ρ) of the films measured with the four-probe technique is 2×10^5 Ω·cm at room temperature). For $[CH(AsF_5)_y]_x$ an R_s value of 200 Ω is obtained, which is also consistent with a bulk resistivity of 5×10^4 Ω·cm.

Capacitance–Voltage (C–V) Data. The capacitance-voltage (C–V) characteristics recorded at various frequencies are given in Figures 3(a) and 3(b), respectively, for undoped and doped polyacetylene. C^{-2} is plotted as a function of the applied voltage in order to assess the acceptor concentration (N_A) and the V_c value according to eq. (1)[11]:

$$C^{-2} = (2/A_j^2 q N_A \epsilon_s)(V_c + V_R) \tag{1}$$

with A_j = junction area; q = electron charge; ϵ_s = semiconductor dielectric constant, taken as 5 in this work, and V_R = reverse applied voltage. This expression is valid in the depletion approximation and in the absence of charge trapping. Considering the parallel plate capacitance, the width of the depletion layer (W) is given by

$$W = \epsilon_s A_j C_0 \tag{2}$$

with C_0 = capacitance in the absence of electrical polarization. The room-temperature values of N_A and W according to eqs. (1) and (2) are given in Table I for undoped polyacetylene.

Short-Circuit Current vs. Wavelength. The short-circuit current action spectrum normalized at constant incident photon intensity (10^{16} photons/cm²·s) is given in Figure 4. The calculated values of I_{sc} have been obtained by application of eq. (5). They will be discussed at the end of this paper. The sample

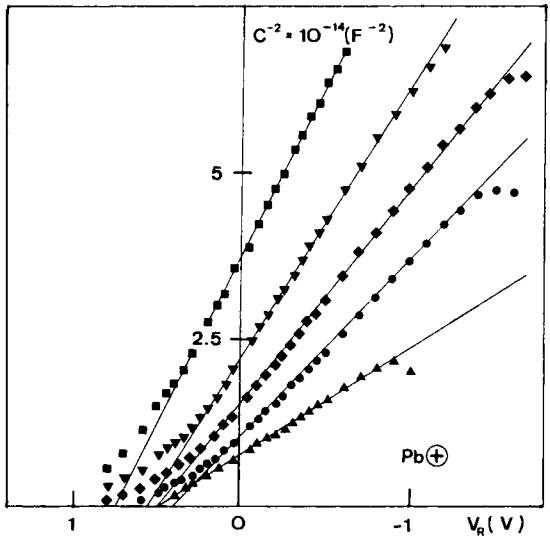

(a)

Fig. 3(a). Capacitance–voltage characteristics at various frequencies of the undoped Pb/$(CH)_x$ cell: (▲) 20 Hz; (●) 360 Hz; (◆) 750 Hz; (▼) 1500 Hz; (■) 3000 Hz.

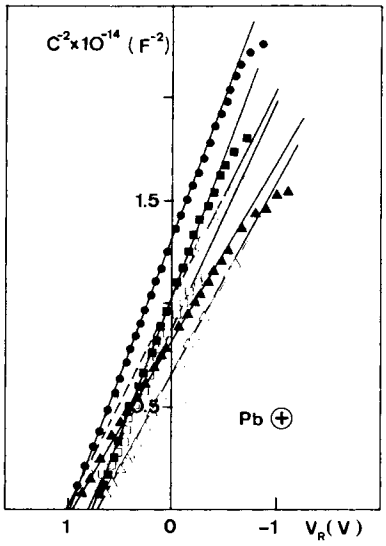

(b)

Fig. 3(b). Capacitance–voltage characteristics at three frequencies of undoped (△,○,□) and doped (▲,●,■) samples: (●,○) 360 Hz; (■,□) 90 Hz; (▲,△) 20 Hz.

is irradiated through the lead contact, and correction for light absorption by the metal has been applied. The largest photocurrents were obtained at ~600 nm and were of the order of 1 μ A·cm^{-2}.

Photovoltaic Data. The photocurrent density–photovoltage characteristics (J_{ph}–V_{ph}) measured by varying the load resistance (R_L) under constant white light illumination (50 mW/cm^2) is shown in Figure 5 for the undoped and doped

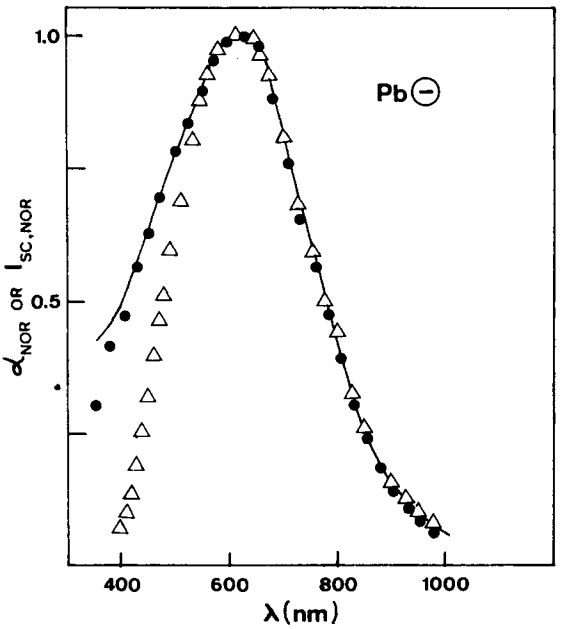

Fig. 4. Visible and near infrared absorption spectrum (●) of a polyacetylene film. Experimental (△) and calculated (—) short-circuit currents (I_{sc}). Absorption coefficients (α) and I_{sc} values are normalized.

films. Characteristic is nearly linear and the fill factor (FF) defined as $P_m/V_{oc}I_{sc}$ with P_m maximum power output is thus ~$51.5 \times 0.61/103 \times 1.23 = 0.25$.

Under the conditions described above, typical values of the photovoltaic data

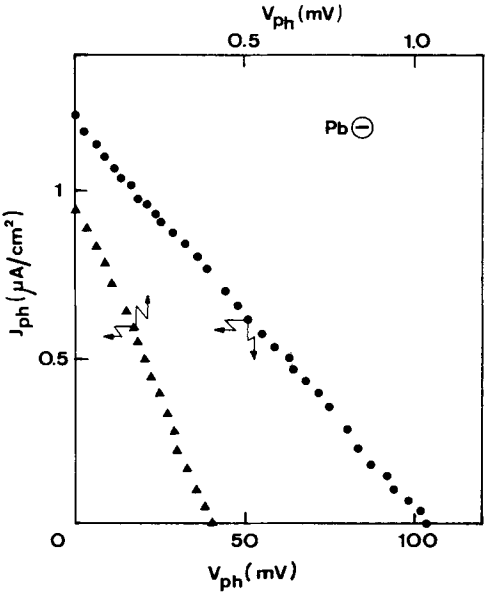

Fig. 5. Photocurrent density (J_{ph}) vs. photovoltage (V_{ph}) of Pb/$(CH)_x$(●) and Pb/$[CH(AsF_5)_y]_x$ photocells (▲). White light illumination; incoming power = 50 mW/cm².

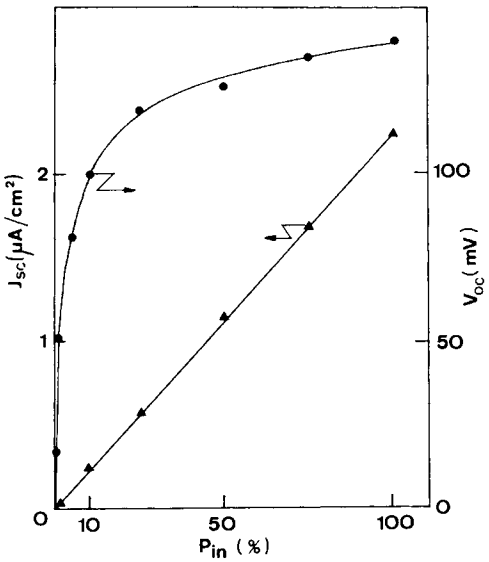

Fig. 6. Plot of the short-circuit photocurrent density (J_{sc}) and the open-circuit photovoltage (V_{oc}) as a function of the incoming light power (P_{in}). 100% corresponds to 50 mW·cm^{-2} (undoped sample).

ranged between 103 and 173 mV for V_{oc} and 1.23 and 2.6 μA/cm^2 for J_{sc}. Similar values were obtained under solar light illumination.

An approximate value of the efficiency of light energy into electrical energy conversion (η) can be estimated according to eq. (3):

$$\eta = V_{oc}J_{sc}\,\mathrm{FF}/P_{in} \tag{3}$$

with P_{in} = incident power/cm^2 (50 mW/cm^2). One finds $\eta \cong 2.2 \times 10^{-4}$%.

Since the currents in the photovoltaic mode are very small, it appears that the low efficiency of the cell does not arise from a series resistance. η is not affected by the film thickness. The quantum yield of carrier collection at 600 nm is 1.33×10^{-2}%.

Short-Circuit Current and Open-Circuit Voltage Dependence on Light Intensity. The short-circuit current density and the open-circuit voltage dependence on white light intensity are given in Figure 6. In these experiments, the incident power was included between 0.5 and 50 mW/cm^2. J_{sc} varies as P_{in} whereas V_{oc} increases logarithmically with the light intensity, which is a usual photocell behavior. As the temperature is raised from 20°C and 45°C, J_{sc} increases (10%) and V_{co} decreases (−2%).

DISCUSSION

As shown in Figure 7, the forward current voltage characteristic is satisfactorily described by the phenomenological equation:

$$J = J_0[\exp[q(V - R_sI)]/nkT] \times [1 - \exp[-q(V - R_sI)]/kT] + (V - R_sI)/R_{sh} \tag{4}$$

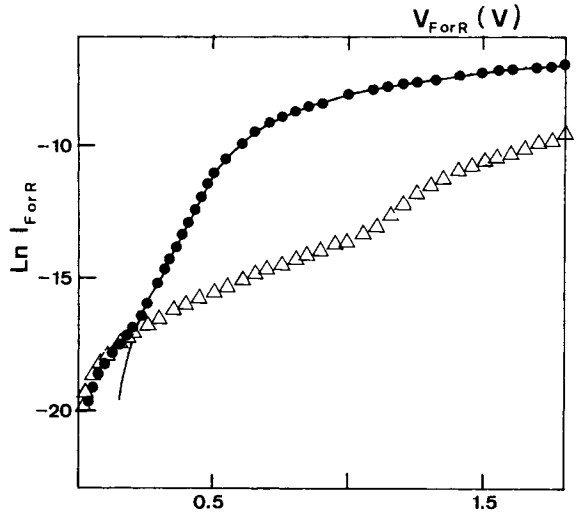

Fig. 7. Natural logarithm of the forward and reverse currents vs. applied potential. Experimental (●,△) and calculated curve (—) by application of eq. (4): (●) Ph ⊖, F; (△) Pb⊕, R.

with R_{sh} being the shunt resistance of the cell and n the perfection factor. In practice, R_{sh} is so large that the last term of eq. (4) may be discarded. Using that equation, the best fit is obtained with $n = 2.2$ and $R_s = 10^3\ \Omega$. It thus appears that the behavior of this Schottky barrier is consistent with the thermoionic-emission theory.

The reverse bias current delivered by the junction is proportional to $\exp(V_c - V_R)^{1/4}$ as expected when image-force lowering of the barrier takes place[11] (Fig. 8).

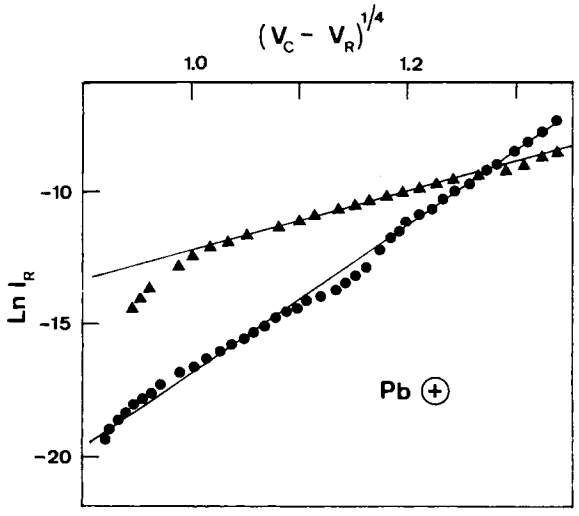

Fig. 8. Effect of the image-force lowering on the Pb/$(CH)_x$ (●) and Pb/$[CH(AsF_5)_y]_x$ (△) barriers. Natural logarithm of the reverse current vs. $(V_C - V_R)^{1/4}$.

TABLE I
Material Parameters Derived from Schottky Barrier Properties for Undoped Polyacetylene

Frequency (Hz)	N_A (cm^{-3})	W (Å)
20	2.79×10^{17}	310
360	1.69×10^{17}	350
750	1.36×10^{17}	430
1500	1.10×10^{17}	530
3000	8.71×10^{16}	690

From the data of Table I, it appears the apparent acceptor density calculated according to eq. (1) depends on the measuring frequency. At higher frequency the calculated N_a value is smaller than at lower frequency.

Presumably, this is due to variable depth traps characterized by different time constants. The same qualitative conclusion can be drawn from the increase of W with increasing frequencies. $N_A = 2.79 \times 10^{17}$ cm^{-3} and $W = 310$ Å are thus the more significant figures.

At the longest wavelengths, the short-circuit current in the photovoltaic mode fits the relationship[12]:

$$I_{sc} = q \times \phi \times N_{ph}[1 - \exp(-\alpha W) + (\alpha/(\alpha + \beta)) \exp(\beta W)] \times [\exp[-(\alpha + \beta)W] - \exp[-(\alpha + \beta)L]] \quad (5)$$

with $\beta^{-1} = L$, the diffusion length of the current carriers, α = absorption coefficient of the polymer (cm^{-1}), ϕ = quantum efficiency of carriers generation, and N_{ph} = light density (quanta/cm^2·s). This is exemplified in Figure 4.

Using iteratively L and W as parameters, a perfect correspondence between the absorbed light and the photocurrent is observed in the range 550–1000 nm for the values $L = 250$ Å and $W = 450$ Å. Thus, the width of the depletion layer estimated from the dependence of the photocurrent with the wavelength is in satisfactory agreement with the W value obtained from the C^{-2} *vs.* V plots at low frequencies.

As far as the diffusion length of the carriers is concerned, a value of 250 Å was also found in a previous study of the indium/*trans*-$(CH)_x$ Schottky barrier.[13] This short diffusion length is again typical of a polymer material having a high density of deep traps.

At wavelengths below 550 nm, I_{sc} is smaller than expected from the application of eq. (5). We tentatively explain this observation in considering that, at short wavelengths, light is partially absorbed by shorter conjugated polyenes whose electronically excited states decay by internal conversion rather than in producing electron–hole pairs.

It must be stressed that the magnitude of the photovoltaic effect is exceedingly small with doped and undoped $(CH)_x$ samples. Furthermore, polyacetylene films display aging effects which are still accelerated by doping with strong electron acceptor or by irradiation with UV and visible light.

The authors are grateful for the valuable technical assistance provided by Mr. Robert Vandeloise. Partial support of this work by the Fonds National de la Recherche Scientifique (FNRS) is acknowledged. One of us (J. K.) thanks the Institut pour l'Encouragement de la Recherche Scientifique dans l'Industrie et l'Agriculture (IRSIA) for the grant of a fellowship.

References

1. E. Vander Donckt, B. Noirhomme, and J. Kanicki, *J. Appl. Polym. Sci.*, **27,** 1 (1982).

2. T. Skotheim, O. Inganäs, J. Prejza, and I, Lundström, *Mol. Cryst. Liq. Cryst.*, **83,** 329 (1982).

3. R. O. Loutfy and C. K. Hsiao, *Polym. Prepr.*, **23,** 237 (1982).

4. E. T. Kang, A. P. Bhatt, E. Villaroel, W. A. Anderson, and P. Ehrlich, *Mol. Cryst. Liq. Cryst.*, to appear.

5. M. Ozaki, D. L. Peebles, B. R. Weinberger, C. K. Chiang, S. C. Gau, A. J. Heeger, and A. G. MacDiarmid, *Appl. Phys. Lett.*, **35,** 83 (1979); M. Ozaki, D. L. Peebles, B. R. Weinberger, A. J. Heeger, and A. G. MacDiarmid, *J. App. Phys.*, **51,** 4252 (1980); B. R. Weinberger, S. C. Gau, and Z. Kiss, *Appl. Phys. Lett.*, **38,** 555 (1981).

6. T. Tani, P. M. Grant, W. D. Gill, G. B. Street, and T. C. Clarke, *Solid State Commun.*, **33,** 499 (1980); T. Tani, W. D. Gill, P. M. Grant, T. C. Clarke, and G. B. Street, *Synth. Met.*, **1,** 301 (1979/80); J. Tsukamoto and H. Ohigashi, K. Matsumura, and A. Takahashi, *Synth. Met.*, **4,** 177 (1982); B. R. Weinberger, M. Akhtar, and S. C. Gau, *Synth. Met.*, **4,** 172 (1982).

7. J. Kanicki, S. Boué, and E. Vander Donckt, *Mol. Cryst. Liq. Cryst.*, **83,** 319 (1982).

8. H. Shirakawa and S. Ikeda, *Polym. J.*, **2,** 231 (1971).

9. A. J. Heeger and A. G. MacDiamid, *The Physics and Chemistry of Low Dimensional Solids*, L. Alcacer, Ed., Reidel, Dordrecht, The Netherlands, 1980, pp. 353–391.

10. Proc. Int. Conf. Low-Dim. Cond., Boulder, Colorado, August 1981, A. J. Epstein and E. M. Conwell, Eds., *Mol. Cryst. Liq. Cryst.*, **77,** 1–356 (1981); Int. Conf. Low-Dim. Synth. Met., Helsingør, Denmark, August 1980, *Chem. Scripta*, **17,** 115–174 (1981).

11. E. H. Rhoderick, *Metal-Semiconductor Contacts*, Clarendon, Oxford, 1980.

12. A. K. Ghosh, D. L. Morel, T. Feng, and C. A. Rowe, Jr., *J. Appl. Phys.*, **45,** 230 (1974).

13. J. Kanicki, E. Vander Donckt, and S. Boué, *Solar Cells*, **9,** 281 (1983).

14. C. Kittel, *Introduction à la physique de l'état solide*, Dunod, Paris, 1972.

Received March 22, 1983
Accepted August 3, 1983